Injectable, self-healing, transparent, and antibacterial hydrogels based on chitosan and dextran for wound dressings

Lei Nie, Qianqian Wei, Meng Sun, Peng Ding, Ling Wang, Yanfang Sun, Xiaoyue Ding, Oseweuba Valentine Okoro, Guohua Jiang, Amin Shavandi

PII: S0141-8130(23)00386-0

DOI: https://doi.org/10.1016/j.ijbiomac.2023.123494

Reference: BIOMAC 123494

To appear in: *International Journal of Biological Macromolecules*

Received date: 9 November 2022

Revised date: 18 January 2023

Accepted date: 27 January 2023

Please cite this article as: L. Nie, Q. Wei, M. Sun, et al., Injectable, self-healing, transparent, and antibacterial hydrogels based on chitosan and dextran for wound dressings, *International Journal of Biological Macromolecules* (2023), https://doi.org/10.1016/j.ijbiomac.2023.123494

Injectable, self-healing, transparent, and antibacterial hydrogels based on chitosan and dextran for wound dressings

Lei Nie[1,*], Qianqian Wei[1], Meng Sun[1,*], Peng Ding[1], Ling Wang[1], Yanfang Sun[2], Xiaoyue Ding[2], Oseweuba Valentine Okoro[3], Guohua Jiang[4,5], and Amin Shavandi[3,*]

[1] College of Life Sciences, Xinyang Normal University (XYNU), Xinyang 464000, China;

[2] College of Life Sciences and Medicine, Zhejiang Sci-Tech University, Hangzhou 310018, China;

[3] Université libre de Bruxelles (ULB), École polytechnique de Bruxelles, 3BIO-BioMatter, Avenue F.D. Roosevelt, 50 - CP 165/61, 1050 Brussels, Belgium;

[4] School of Materials Science and Engineering, Zhejiang Sci-Tech University, Hangzhou, 310018, China;

[5] International Scientific and Technological Cooperation Base of Intelligent Biomaterials and Functional Fibers, Zhejiang Sci-Tech University, Hangzhou, 310018, China;

*** Corresponding author I: Dr. Lei Nie**

Post address: College of Life Sciences, Xinyang Normal University (XYNU), Xinyang 464000, China. Tel: +86-13600621068.

ORCID: 0000-0002-6175-5883

E-mail address: nieleifu@yahoo.com; nielei@xynu.edu.cn

*** Corresponding author II: Dr. Meng Sun**

Post address: College of Life Sciences, Xinyang Normal University (XYNU), Xinyang 464000, China.

E-mail address: sunmeng2010abc@163.com

*** Corresponding author III: Dr. Amin Shavandi**

Post address: BioMatter unit - École polytechnique de Bruxelles, Université Libre de Bruxelles, Avenue F.D. Roosevelt, 50 - CP 165/61, 1050 Brussels, Belgium

E-mail address: amin.shavandi@ulb.be

Abstract

One major shortcoming of biopolymeric based wound dressing so far is the lack of an integrated multi-functional system that could provide suitable mechanical strength, fast self-healing, transparency, antibacterial and antioxidant effects. Benefiting from the dynamic and rapid reaction between glycidyl trimethyl ammonium chloride-graft- chitosan (QCS) and aldehyde-dextran (ODex) under physiological conditions, we designed hydrogels (QCS-ODex) with fast *in situ* gel-forming (< 70 s), porous structure (300-350 μm), stable storage modulus and the loss modulus, suitable swelling capacity (2.465 folds of chitosan), tissue adhesion, transmission property, free radical scavenging capacity, good self-healing behavior, and injectability, inherent antibacterial (against *E. coli* and *S. aureus*) and biocompatibility. Furthermore, Baicalein could be *in situ* encapsulated into QCS-ODex hydrogels, and the release behaviour of Baicalein could be regulated by adjusting the ratio of QCS and ODex. The Baicalein-loaded QCS-ODex hydrogel further facilitated free radical scavenging and antibacterial bioactivities due to the cooperative therapeutic effects between QCS-ODex and Baicalein. This study may provide new insights into designing multi-functional QCS-ODex hydrogels with multiple therapeutic effects as a wound dressing.

Graphical Abstract

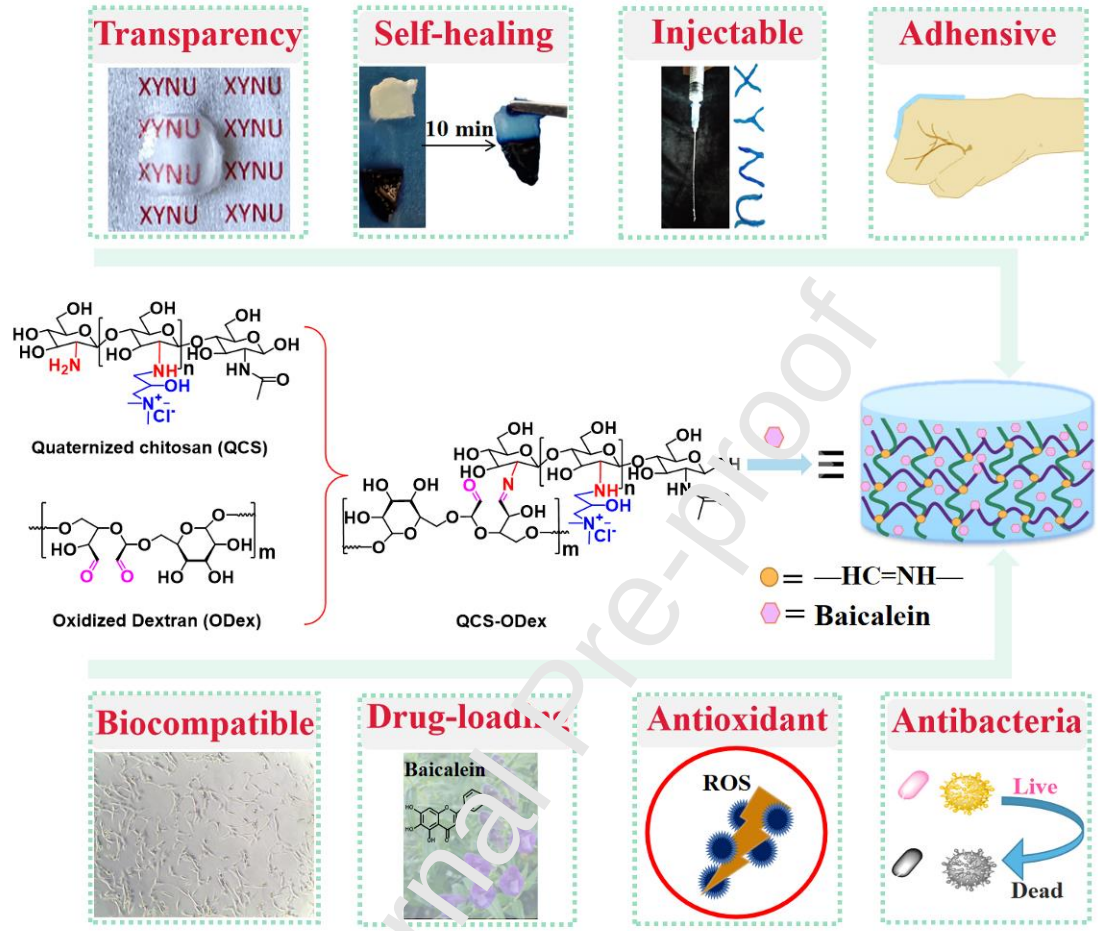

Keywords: Quaternized chitosan; oxidized dextran; Schiff base; hydrogels; wound dressings.

1. Introduction

Wound healing is the most important restorative process for skin injury when the skin layers are cut, torn, or punctured by external stimulation or trauma, and it will bring long-term pain and mental burden to patients [1-4]. Thus, an appropriate wound dressing is necessary. Several wound dressings, such as semipermeable membranes, gauze, foam, hydrocolloids, nanoparticles, and cryogel have been developed to promote wound repairs [5-9]. However, most existing dressings do not provide a multi-functional system with

suitable mechanical, antibacterial and antioxidant properties. Therefore, developing a dressing with injectable, self-healing and transparency properties for wound treatment is necessary [10, 11]. The hydrogel was seen as a more suitable candidate for wound dressings because of its soft, porous and high-water content. It is beneficial for absorbing abundant exudates or blood, maintaining a comparable moist, cool and clean environment and keeping good O_2 exchange and water permeability in skin defect sites to promote wound healing and relieve patients' pain [12-16]. Hydrogels can be particularly useful in wound dressings since they are able to not only hydrate wounds and re-hydrate eschar but are capable of promoting autolytic debridement [17]. Similarly, highly transparent hydrogels are convenient for monitoring the healing process and diagnosing wounds in real time for giving on-demand therapy [18, 19]. Many biopolymers were used to fabricate hydrogels as wound dressings, including chitin, chitosan, cellulose, collagen, silk fibroin, alginate, gelatin, fucoidan, hyaluronic acid, and so on [20-24].

In addition, self-healing and *in situ* injectable hydrogels with adhesive ability can match and completely fill any shaped wounds, especially for those motion wounds, providing a sealed environment to protect wounds, isolate external bacterial clones and decrease the risk of wound infection [2, 25, 26]. Schiff base bond (-CH=NH-) is a dynamic covalent bond suitable for fabricating dynamic hydrogels with self-healing, shape memory, *in situ* gelation or injection in physiological environments [27]. Among biopolymers, chitosan (CS) is biocompatible, nontoxic, biodegradable biopolymer with antioxidative, antibacterial, anti-inflammatory and hemostasis characteristics, making it suitable for wound treatment [28-30]. Some reports have proved that grafting quaternary ammonium salt on the chitosan

polymer chain can enhance its water-solubility and antibacterial activity [6, 31, 32]. Quaternized chitosan (QCS)-based hydrogels with high transparency, self-healing, injectable, and inherent antibacterial characteristics, simultaneously, have been rarely reported as wound dressings for wound healing [6, 27].

Due to the benefits of employing hydrogels in wound healing applications, several studies have explored the viability of using several hydrogels in wound healing applications. For instance, in the study by *et al.* [33], a hydrogel based on Methacrylated kappa-carrageenan (KaMA) and containing dopamine functionalized graphene oxide (GOPD), was prepared and employed in wound healing. The study showed that the introduction of GOPD led to an improvement in the shear-thinning behavior of the hydrogel for improved injection properties [33]. The introduction of GOPD in the hydrogel was also shown to promote the proliferation and spreading of fibroblasts, which will further enhance wound healing potential when applied [33]. In another study by Annabi *et al.* [34], a sprayable composite hydrogel was formulated using methacrylated gelatin (GelMA) and methacryloyl-substituted recombinant human tropoelastin (MeTro) to synthesize a sprayable MeTro/GelMA composite hydrogel. The composite hydrogel was determined to have favourable mechanical properties and antimicrobial activities against Gram (+) and (−) bacteria, when conjugated with the antimicrobial peptide Tet213 [34]. The study was able to demonstrate the potential of employing hydrogel in promoting sutureless wound closure since it can reduce the risk of infection and enhance the healing of chronic wounds [34]. In line with the existing interest in the exploration of hydrogels for wound healing applications, the present study has investigated the development of a series of glycidyl trimethyl ammonium

chloride-graft-chitosan (QCS)/aldehyde-dextran (ODex) Schiff base hydrogels named QCS-ODex. The hydrogels have been prepared by leveraging the reaction between the chitosan amino group and the dextran aldehyde group. It must be noted that chitosan was employed as the base biomaterial due to its unique hydrophilic properties, biocompatibility and ability to be degraded by human enzymes [35]. Notably, chitosan also has favourble bacteriostatic, and hemostatic properties,while also presenting the ability to enhance the rate of blood clotting at the wound site due to its ability to bind with red blood cells [35]. The use of chitosan in wound healing applications is therefore widely investigated. For instance Caetano *et al.*, [36] investigated the effect of applying a hydrogel of chitosan–alginate membrane on a cutaneous wound in rats and determined that the hydrogel limited the risk of infection and reduced the amount of inflammatory infiltrate, at the wound site, while simultaneously increasing the proliferation of fibroblast cells. Similarly, Howling *et al.* [37] showed that the using of chitosan based hydrogel in wound healing led to an improvement in fibroblast proliferation at wound site,for improved wound healing overall.

The present study, therefore, also investigated the effects of the substitution degree (DS) of QCS on the self-healing, antioxidant and antibacterial multifunctions of the transparent injectable hydrogel. Moreover, after loading the drug, Baicalein, the hydrogels (B-QCS-ODex) exhibited increased antioxidant and antibacterial activities. Baicalein, (i.e. 5,6,7-trihydroxyflavone,) was added to the hydrogel due to its reported favourable anti-inflammatory, antiviral and antioxidant properties. Notably, Baicalein has also been reported to have the potential to inhibit the growth of some tumours [38]. The designed QCS-ODex hydrogels possess excellent physiochemical and biophysiological properties as

potential wound dressings.

2. Materials and method

2.1 Materials

Chitosan (CS, 80~95% deacetylation degree and 200-800 cP viscosity), glycidyl trimethyl ammonium chloride (GMTAC, 95%), sodium periodate ($NaIO_4$, 99.5%), dextran (Dex, Mn=10000), Baicalein were purchased from Sigma-Aldrich Co., Ltd. Millipore water was prepared using a Milli-Q50 SP Reagent Water System (Millipore Corporation, USA). All chemicals and solvents purchased were used as received without further purification.

2.2 Synthesis of glycidyl trimethyl ammonium chloride-graft-chitosan (QCS)

QCS was synthesized according to a previous report as previous report with some modifications [6]. 8.0 g CS and 7.2 g GTMAC were suspended in 300 mL deionized (DI) water in a three-necked flask. Then the liquid was stirred at 80 °C for 36 h with a reflux operation. After that, the mixture was dialyzed for 3 days in DI water to remove undissolved polymers. Moreover, fresh DI water was changed three or four times a day. The final product was obtained by freeze-drying, named QCS1. Following the above method, 7.2 g GTMAC was changed to 14.4 g GTMAC to synthesize QCS2. The degree of substitution (DS) of QCS was determined by ^{1}H nuclear magnetic resonance (^{1}H NMR, Bruker 600 MHz).

2.3 Synthesis of aldehyde-dextran (ODex)

ODex was synthesized according to reference with modification [39]. 3.0 g sodium periodate ($NaIO_4$) (dissolved in 80 mL DI water) was added to 320 mL of dextran (Dex) solution (1.25 wt% (w/v)) and continuously stirred at 25 °C, shielded from light. 24 h later,

the mixing product was subsequently dialyzed using DI water for 3 days. Finally, the pure ODex was obtained by lyophilization for 3 days. The obtained white ODex were stored in a dark and dry environment.

2.4 Preparation of QCS-ODex hydrogels

QCS1, QCS2 and ODex polymers were dissolved in DI water to form 3 wt% (w/v), 3 wt% (w/v) and 12.5 wt% (w/v) solutions, respectively. QCS1-ODex-31 and QCS1-ODex-61 hydrogels were prepared by mixing QCS1 and ODex solutions in a ratio of 3:1 (v/v) and 6:1 (v/v) at 25 °C, respectively. QCS2-ODex-31 and QCS2-ODex-61 hydrogels were prepared with a similar method for QCS1-ODex-31 and QCS1-ODex-61 hydrogels, except that using QCS2 solution as substrate. The gelation time of hydrogels was evaluated using the tube inversion method [40, 41]. 3 wt% (w/v) QCS solution was added into a vial, and then 12.5 wt% (w/v) ODex solution was added at room temperature (RT). The sol-to-gel transition of the mixture was investigated every 10 s using the tube inversion method, and the gelling time of hydrogels was recorded.

2.5 Preparation of Baicalein loading QCS-ODex hydrogels

QCS1, QCS2 and ODex polymers were dissolved in DI water to form 3 wt% (w/v), 3 wt% (w/v) and 12.5 wt% (w/v) solutions, respectively. Baicalein was weighed and dissolved in ethanol to prepare 5 mg/mL baicalein solution. After evenly mixing 3 wt% (w/v) QCS1 solutions and 5 mg/mL baicalein solution, 12.5 wt% (w/v) ODex solution was added into the mixture according to the ratio of forming QCS1-ODex-31 hydrogel and QCS1-ODex-61 hydrogel, respectively. After allowing complete gelation, the drug-loaded hydrogels formed, and the drug was *in situ* encapsulated in the hydrogels. Then, the drug-loading hydrogels

were obtained and named B-QCS1-ODex-31 hydrogel and B-QCS1-ODex-61 hydrogel, respectively. Following the same method, 3 wt% (w/v) QCS1 was changed to 3 wt% (w/v) QCS2, and the B-QCS2-ODex-31 and B-QCS2-ODex-61 hydrogels were obtained (Table S1).

2.6 ^{1}H nuclear magnetic resonance (^{1}H NMR) analysis

The tested polymers (CS, QCS, Dex, and ODex) were dissolved in D_2O, respectively, and the dissolved samples were transferred into the nuclear magnetic tubes. The optimal height of the sample in the NMR tube was 4 cm. H-spectrum then tested the prepared samples on the nuclear magnetic resonance spectrometer (^{1}H NMR, 600 MHz, NMR spectrometer, JEOL ECZ600R/S3).

2.7 Fourier-transform infrared spectroscopy (FT-IR) analysis

The structure of QCS and ODex polymers, and the presence of specific chemical groups in QCS-ODex hydrogels were confirmed by Fourier-transform infrared spectroscopy (FT-IR, PerkinElmer Spectrum 2). The FT-IR spectra were obtained within the range between 500 and 4000 cm^{-1} with a resolution of 1 cm^{-1}, with each spectrum averaged over 64 scans.

2.8 X-ray diffractometer (XRD) analysis

An X-ray powder diffractometer (XRD, Rigaku Smartlab 9 kW), operated at 45 kV and 200 mA with Cu Kα radiation (λ = 1.5406 Å) and a spinning sample holder, was used to obtain XRD patterns of QCS-ODex hydrogels. Data were acquired in the 2θ range of 5-90° at a step increment of 10°.

2.9 Scanning electron microscope (SEM) analysis

A field emission scanning electron microscope (SEM, Hitachi Regulus8220) was used to

observe the morphologies and the pore size of the freeze-dried QCS-ODex hydrogels. Before observation, the surface of the hydrogels was sprayed with a platinum layer, sustaining 40 s.

2.10 Rheological properties analysis

The rheological performance of the QCS-ODex hydrogels was evaluated by a TA rheometer (DHR-2, USA) with 1% constant strain and a constant frequency of 10 rad/s at 37 °C [42]. Store modulus (G') and loss modulus (G") were measured using a 40 mm diameter and 1 mm clearance aluminium low inertia parallel plate. In order to avoid evaporation of water from the sample during the test, the edge of the fixture was sealed using glycerin.

2.11 Transparency analysis

The transmittance of the QCS-ODex hydrogels was recorded by the photograph and tested with an Ultraviolet-visible Spectroscopy (UV-Vis, PerkinElmer, Lambda 950), and the data of samples were recorded in the range of 200-800 nm at 298 K.

2.12 Swelling analysis

The freeze-dried QCS-ODex hydrogels were firstly weighted (W_A) before equilibrating in DI water at RT. Hydrogels were taken out from the water at the pre-set time intervals, and the excess water on the hydrogel surface was removed with filter paper [31]. Then, the hydrogels were weighed (W_B). The swelling rate (SR) was calculated as:

$$\text{SR}\ (\%) = \frac{W_B - W_A}{W_A} \times 100\%$$

Where W_A and W_B represented the initial weight of the dried hydrogels and the weight after swelling equilibrium, respectively. The test of each hydrogel sample group was repeated three times.

2.13 Self-healing analysis

Macroscopic self-healing experiment: The hydrogel was cut into two pieces. One piece was stained by dimethyl blue, and the other made no change. And then, the two pieces were put together for 10 min to allow them to heal into a complete hydrogel at RT [15].

Quantitative self-healing test: The hydrogel was placed between 20 mm parallel plates with a gap of 1000 μm on a TA rheometer plate, and the periphery was sealed by silicone oil to prevent the evaporation of water. Strain amplitude sweep tests (γ = 0.1%-600%) were operated at a fixed angular frequency (10 rad/s) at 25 ^{o}C to record the value of the critical strain region. Amplitude oscillatory strains were switched from small strain (γ = 1.0%) to subsequent large strain (γ = 400%) with 100 s for every strain interval to determine the self-healing ability of the hydrogels, and three cycles were carried out [43].

2.14 Injectability analysis

The hydrogels were loaded into a syringe (with an inner nozzle diameter of 1.5 mm) and put out of the injector fluently (**Supporting Video 1**). The shear flow property of the hydrogel was recorded by a TA rheometer. Oscillation-frequency experiments were conducted under a constant strain of 1%, varying the shear rate from 0.1 rads/s to 100 rad/s at 25 °C.

2.15 Adhesive properties analysis

The hydrogel's adhesive performances were determined by directly connecting the skin with different actions such as arm, finger, and finger joints (**Supporting Video 2**).

2.16 *In vitro* Baicalein release

In vitro release tests of the QCS-ODex hydrogels loaded with Baicalein were carried out by immersing drug-loaded samples in a definite volume (5 mL) of PBS (pH = 7.4). At

predetermined time intervals, 0.5 mL of the release buffer was removed for analysis by a UV-Vis spectrometer at 275 nm, and 0.5 mL of fresh buffer was added to the tube to retain a constant volume. All sample groups were performed three times.

2.17 Antioxidant analysis

Antioxidant tests of QCS and ODex polymers, QCS-ODex hydrogels and Baicalein-loaded QCS-ODex hydrogels were evaluated using the stable 1,1-diphenyl-2-picrylhydrazyls (DPPH) free radical. Polymers, QCS-ODex hydrogels and baicalein loading QCS-ODex hydrogels (2 mg) were added to DPPH solution (2 mL, 0.1 mM) with ethyl alcohol, respectively. The mixture was stirred and incubated in a dark place for 30 min. Then, the wavelength of DPPH was scanned using a UV-Vis spectrophotometer from 200 nm to 800 nm. The degree of light absorption was measured at 517 nm, and the following equation calculated the scavenging ratio:

$$DPPH\ scavenging\ (\%) = \frac{A_0 - A_1}{A_0} \times 100\%$$

Where A_0, and A_1 are the absorption of the blank (DPPH + ethanol) and the absorption of the sample (DPPH + ethanol + sample), respectively [44].

2.18 Antibacterial activity evaluation

The antibacterial actions of the hydrogels against Gram-negative *E. coli* (ATCC 25922) and Gram-positive *S. aureus* (ATCC 6538) were determined according to the publication [45-47].

Hydrogels surface antibacterial activity: In brief, QCS-ODex hydrogels were cut into disks with 4 mm diameter and 1.5 mm thickness and sterilized by UV light radiation for 2 h. 100 μL of bacteria suspension with a concentration of 10^7 CFU mL^{-1} were spread onto a 90

mm-diameter nutrient agar (NA) plate and incubated with the hydrogel disks for 24 h in a humidified incubator at 37 °C. The inhibition zones of each sample were recorded. After that, these hydrogel samples were transferred to a new NA medium plate which was covered with bacterial suspension (100 μL) and incubated for another 24 h [48].

Hydrogels in Luria Bertani (LB) agar liquid medium antibacterial activity: Briefly, 0.002 g hydrogels were added to a glass tube with 10 mL LB medium and 10 μL the diluted bacteria suspension to culture growth at 37 °C for 12 h. 24 h. Lastly, a UV-Vis spectrophotometer tests and records optical density at 600 nm (OD600). The glass tube with 10 mL LB medium and 10 μL the diluted bacteria suspension without the hydrogel as a blank control group. The antibacterial ratio was calculated by the following equation:

$$Antibacterial\ ratio\ (\%) = \frac{K_b - K_s}{K_b} \times 100\%$$

Where K_b, and K_s are the absorption of the blank control group and the absorption of the sample group, respectively. The tests were repeated three times for each group.

0.002 g hydrogel was added to a glass tube with 10 mL LB medium and 10 μL the diluted bacteria suspension to culture growth at 37 °C for 24 h. The glass tube with 10 mL LB medium and 10 μL the diluted bacteria suspension without the hydrogel as a blank control group. Then, 10 μL bacteria suspension was transferred to silica wafers, fixed by 50 % glutaraldehyde for 24 h at 4 °C, and dehydrated for 10 min with 50%, 70%, 90%, and 95% ethanol sequentially, and left for 30 min in 100% ethanol. The dried bacteria were sprayed with a platinum layer and observed by SEM [18].

2.19 Biocompatibility evaluation

In vitro cytotoxicity assay: The cytotoxicity of hydrogels was assessed by cell counting

Kit-8 (CCK-8) assay. Briefly, mouse fibroblast (NIH-3T3) cells (CRL-1658^{TM}, ATCC) were grown in Dulbecco's modified Eagle's medium (DMEM) with 10 % fetal bovine serum, 100 U mL^{-1} penicillin, and 100 μg mL^{-1} streptomycin under a humidified incubator containing 5% CO_2 at 37 °C, according to ATCC instruction. The cells at passage 5 were used for the next experiments. NIH-3T3 cells were seeded in copolymer solutions and on hydrogels surface in a 96-well plate and incubated for 24 h, 48 h and 72 h in a humidified incubator. The cells of the control group were cultured in media without a hydrogel sample. The control group and each sample were tested in triplicate. On pre-set days (1, 2, and 3 days), 10 μL of CCK-8 reagent was added to each well and incubated for 2 h in an incubator. After that, each well liquid was transferred into a new 96-well plate, and its fluorescence was read using a microplate reader (SpectraMax 190, Molecular Devices) at 450 nm wavelength, according to the manufacturer's instructions. The cell morphology co-cultured with the hydrogels extract for 24 h was observed using phalloidin-FITC and 4'6-diamidino-2-phenylindole (DAPI, Thermo Scientific^{TM}) staining by an inverted phase microscope and a laser confocal fluorescence microscope (CLSM, Leica TCS SP5 II, Germany).

Cell migration assay: NIH-3T3 cells were seeded at the 96-well plate and co-cultured with 100 μL hydrogels extract at 37 °C for 24 h in an incubator. After that, the liquid was removed, scratched a straight line on the cell monolayer with a 10 μL pipette sharp tip and washed twice using PBS solution to remove the damaged cells away from the wells. Next, the wells were added to 100 μL of fresh medium and recorded in the original straight line. Subsequently, the 96-well plate was placed in an incubator for 8 h [28]. The change of scratch straight line was obtained via an optical microscope and analyzed by ImageJ software.

2.20 Statistic analysis

The data were expressed as mean ± standard deviation (SD) of three determinations. The data were analyzed using one-way ANOVA, and P value < 0.05 was considered statistical significance.

3. Results and discussions

3.1 Synthesis and characterizations of QCS, ODex and QCS-ODex hydrogels

The schematic representation of QCS, ODex polymers and QCS-ODex hydrogels is shown in **Fig. 1a**. QCS polymer was synthesized by grafting glycidyl trimethyl ammonium chloride (GMTAC) on the CS chain (**Fig. S1a**). In ^{1}H NMR spectra of CS, QCS1 and QCS2, two obvious characteristic peaks of proton at 3.2 and 3.5 ppm were attributed to trimethylammonium and –NH–CH_2– group, respectively (**Fig. 2a**) [49]. FT-IR spectra of QCS1 and QCS2 showed the characteristic peak at 1475 cm^{-1}, assigning to the methyl group (C-H) bending of the trimethylammonium group from GMTAC (**Fig. 2c**). These results indicated that quaternary ammonium group was grafted onto the CS chain successfully [31].

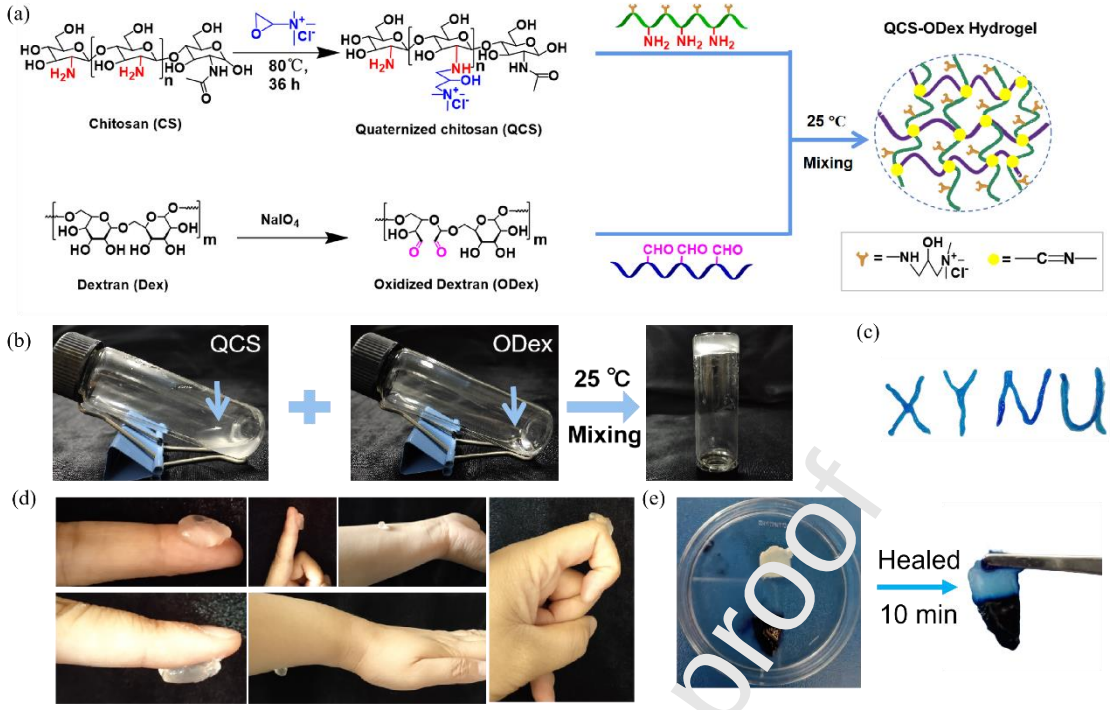

Figure 1. Schematic of QCS-ODex hydrogel synthesis. (**a**) The synthesis procedure of QCS-ODex hydrogel. (**b**) Photographic images of QCS and ODex solution and free-standing QCS1-ODex-61 hydrogel. (**c**) The injectable of the hydrogel via an injector. The hydrogel was stained with methylene blue. (**d**) Photographs of the adhesive of the hydrogel QCS2-ODex-31 on a finger, arm and joint. (**e**) The self-healing was displayed by QCS1-ODex-61 hydrogel (The colored hydrogel was stained by methylene blue).

The aldehyde functional group of ODex was prepared via an oxidation-reduction reaction with $NaIO_4$ (**Fig. S1b**). ^1H NMR spectra of Dex and ODex from 3.2 to 5.4 ppm corresponding to the hydroxyl and methylene protons in dextran (**Fig. 2b**) [50]. The new peak of 9.7 ppm was attributed to the aldehyde functional group of ODex [43]. In FT-IR spectra of Dex and ODex, a new weak absorption peak appeared at 1731 cm^{-1} in ODex, corresponding to the aldehyde functional group, which showed the formation of the aldehyde group of

ODex (**Fig. 2d**) [51].

QCS-ODex hydrogels were synthesized by mixing QCS and ODex solutions at room temperature (**Fig. 1b** and **Fig. S2**). Amino and aldehyde groups formed dynamic imine linkage *in situ*. A new absorption peak at 1644 cm^{-1} in FT-IR spectra of QCS-ODex hydrogels was the stretching vibration of the –C=N– bond (**Fig. 2e**), revealing that Schiff base bonds existed in prepared QCS-ODex hydrogels [27]. Additionally, the aldehyde group peaks at 1731 cm^{-1} of ODex weakened or disappeared in the spectrum of QCS-ODex hydrogel, indicating that the aldehyde group of ODex was consumed when formed hydrogels by Schiff base reaction.

The gelation time is a significant indicator of wound dressings' practical application to the wound area with *in situ* gel formation [52]. The gelation time was approximately 17 s, 43 s, 57 s and 69 s for QCS1-ODex-61, QCS1-ODex-31, QCS2-ODex-61, and QCS2-ODex-31 hydrogels, respectively (**Fig. 3a**). QCS1-ODex-61 hydrogel displayed the fastest gelling time compared to other hydrogels, which mainly due to that more amino groups left in OCS1 than QCS2, further causing more Schiff base reactions with ODex. Notably, the gelation time (17 s) of the best-performing QCS1-ODex-61 hydrogel can be shown to be competitive when compared to the gelation time (30 s) of the recently reported and novel ultrashort gelation of the multi-functional hydrogel/composite that was developed using self-catalytic $Fe^{3+/}$Tannic acid-cellulose nanofibers [53]

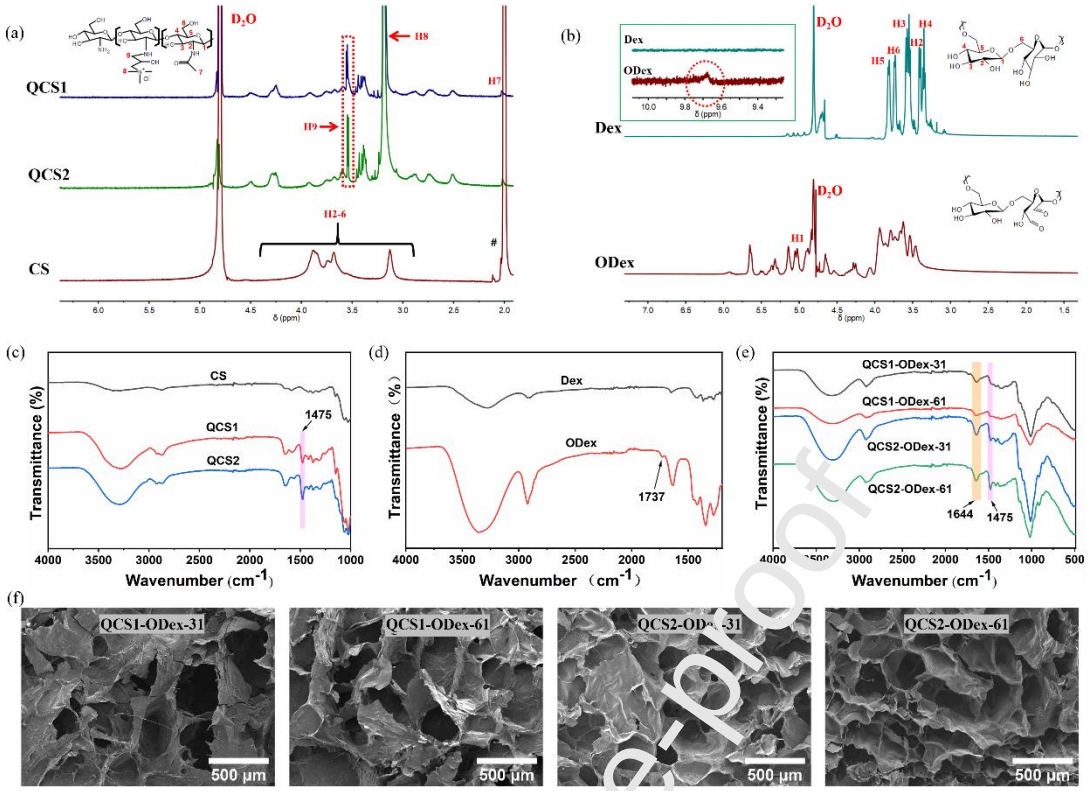

Figure 2. Characterization of QCS and ODex polymers, and QCS-ODex hydrogels. The ^{1}H NMR of (**a**) QCS1, QCS2, CS (in D_2O) ($^{\#}$: Acetic acid.) and (**b**) Dex, ODex (in D_2O). FT-IR spectra of (**c**) CS, QCS1, and QCS2; (**d**) Dex and ODex; (**e**) QCS-ODex hydrogels. (**f**) SEM images of QCS-ODex hydrogels.

3.2 Adhesive property

QCS-ODex hydrogels showed good adhesiveness on human skin, especially in dynamic areas with frequent activity, such as joints (**Fig. 1d** and **Supporting Video 2**). For QCS-ODex hydrogel, the adhesion was assigned to the positively charged amino groups and quaternary cation of QCS, and hydrogen bonds, hydrophobic interactions and electrostatics between QCS and the surrounding skin tissue surface [54].

3.3 Morphology

The uniformitarian and interconnected morphology of these QCS-ODex hydrogels were observed with a scanning electron microscope (SEM) shown in **Fig. 2f**. QCS-ODex hydrogels possessed more regularity and homogeneous pores than QCS1, QCS2 and ODex hydrogels (**Fig. S3**). The average pore diameter of QCS-ODex was between 300-350 μm (**Fig. S4**). The uniform porous structure of hydrogels is beneficial for absorbing and storing excess exudate from the wound area, and ensuring oxygen permeability for wound healing [55]. The enhanced presence of pores in the hydrogels is expected when compared to the morphology of other hydrogels employed in wound dressing in the literature. For instance, novel hydrogels of Poly(ε-caprolactone-co-lactide)/Poloxamer (PLCL/Poloxamer) nanofiber and Dextran/Gelatin hydrogel [56] and keratin nanofiber and gelatin-methacrylate hydrogel [57] were also shown to have a well-interconnected morphology with enhances mass (i.e. nutrient, water etc., air) transfer for the proliferation of fibroblasts and improved wound healing overall.

3.4 Mechanical properties

Considering the practical application in the wound healing field, the mechanical property of the hydrogels was evaluated. The storage modulus (G') and the loss modulus (G'') of hydrogels were recorded over time at 1 rad·s^{-1} frequency (**Fig. 3b**). G' of QCS1-ODex-31 and QCS1-ODex-61 hydrogels was approximately 3000 Pa, but G' of QCS2-ODex-31 and QCS2-ODex-61 hydrogels was 700 Pa. Obviously, QCS1-ODex hydrogels had better mechanical properties than QCS2-ODex hydrogels, which mainly due to that the increased cross-linking density caused by increased Schiff base bonds, could improve the mechanical strength and structural stability of hydrogels [58, 59].

3.5 Swelling behavior

Hydrogels with good absorption capacity can absorb excess exudate from the wound area, reducing the damage from the fibrinolytic enzyme in wound effusion and providing a moist environment for wound tissue to promote wound healing [13, 60]. In **Fig. 3c**, QCS2-ODex-31 and QCS2-ODex-61 hydrogels exhibited a high swelling ratio of 2334 ± 374%, and 2465 ± 590%, respectively, after 100 min of immersion in DI water. In contrast, QCS1-containing hydrogels (QCS1-ODex-31 and QCS1-ODex-61) exhibited lower swelling ratios of 1421±348%, and 1418±339%, respectively. This decrease suggests that the interconnected network and macroporous structure of QCS2-containing hydrogel will favour water uptake.

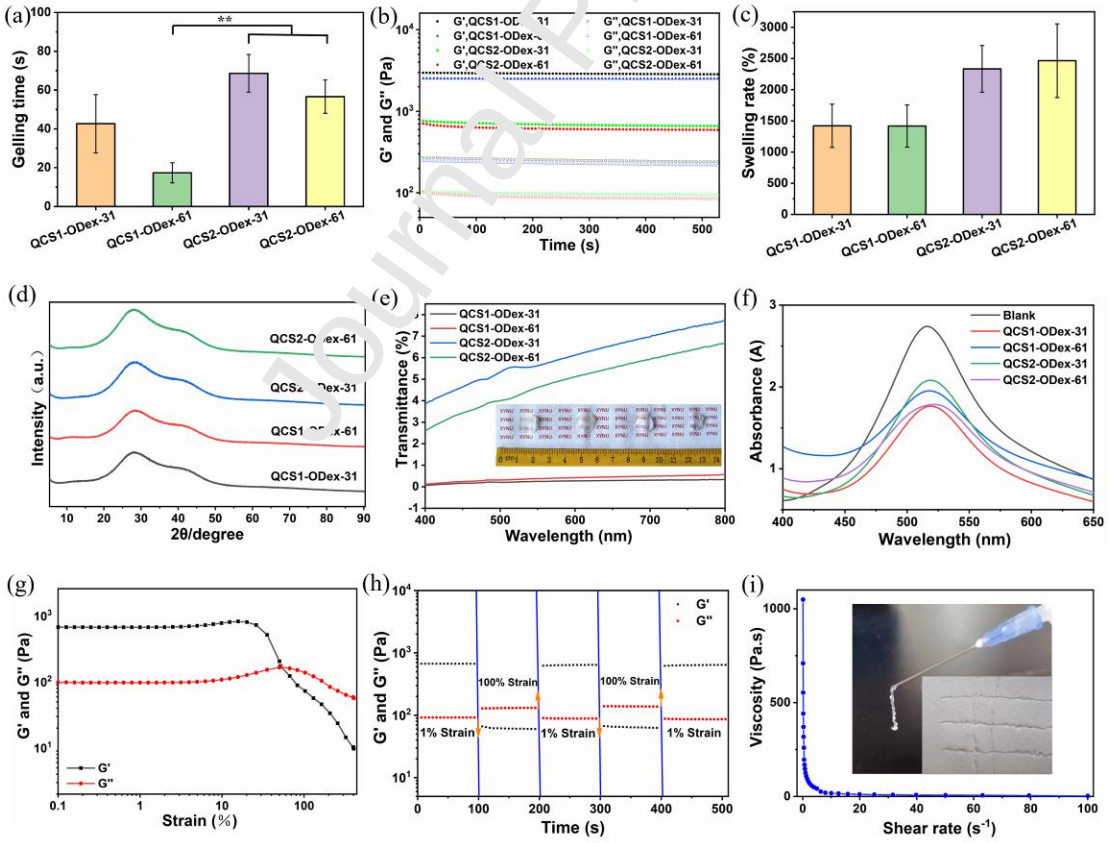

Figure 3. Physical characterization of QCS-ODex hydrogels. (**a**) Gelling time of QCS-ODex

hydrogels (**p < 0.01). (**b**) The storage modulus (G') and the loss modulus (G'') of QCS-ODex hydrogels. (**c**) Swelling property of QCS-ODex hydrogels in DI water. (**d**) XRD test of wet QCS-ODex hydrogels. (**e**) The transparency test of the hydrogels. (**f**) UV-Vis spectra of DPPH scavenging. (**g**) G' and G'' for the strain scan of QCS2-ODex-31 hydrogel. (**h**) The self-healing property of the hydrogel was tested by a rheometer (QCS2-ODex-31 hydrogel was subjected to alternate strain from 1% to 100%). (**i**) Viscosity dependence on the shear rate of QCS2-ODex-31 hydrogel (inset photograph representative that the hydrogel was injected by a syringe). The oscillation-frequency experiments were conducted under a constant strain of 1%, varying the shear rate from 0.1 rad/s to 100 rad/s at 25 °C.

3.6 Crystallographic and transmission properties

XRD traces for all hydrogel samples can be seen in **Fig. 3d**. All hydrogel exhibited similar features, with the main peak at approximately 32.08° and a weak and low peak at 43°, showing crystallinity and ease with high-transparency gelation forming [18]. QCS1-ODex hydrogel exhibited peaks in the same locations but with different peak ratios compared to QCS2-ODex hydrogels. For QCS2-ODex-61 hydrogel, the peak at 32.08° exhibited the highest intensity, showing that it may possess the highest transparency. The crystalline structure and the state of the intermolecular reaction field of hydrogels are governed by their network structure, which was greatly influenced by the cross-linking density [61]. The morphology and transparent properties of hydrogel were also greatly influenced by its cross-linking density (**Fig 2f** and **Fig 3e**) [62]. The high crystallinity of QCS2-ODex-61 hydrogel was due to the higher content of GMTAC on the QCS chain, which increased the

cross-linking density in its hydrogel network. The dried hydrogels displayed the same peaks without any new changes compared to wet hydrogels (**Fig. S5**).

A highly transparent hydrogel will facilitate direct observation and real-time monitoring of wound recovery for the doctor and patient, reducing nursing time and procedures and achieving on-demand therapy [63, 64]. Both QCS2-ODex-31 and QCS2-ODex-61 hydrogels exhibited higher light transmission rates from 400 to 800 nm compared to QCS1-ODex hydrogels, whose crystallinity and content of GMTAC was lower (**Fig. 3e**). The characteristics of the different hydrogel formulations are well highlighted in **Fig. 3**, inset graph. **Fig. 3** shows that higher concentrations of QCS2 resulted in the higher transparency of hydrogels, and QCS2 also possessed higher transparency than QCS1. The conclusion also could be presented by the results of the transparency test of QCS1, QCS2 and ODex by a UV-Vis spectrum (**Fig. S6**). The transmittance of QCS2 is higher than QCS1, and the transmittance of ODex was the highest.

3.7 Self-healing and injectable properties

The self-healing ability can effectively prolong the lifespan of wound dressings [49]. The QCS2-ODex-31 hydrogel was selected as the representative group to show the self-healing property of these QCS-ODex hydrogels. In the macroscopic self-healing performance test, after cutting into two disks and put together for 10 min at 25 °C, the hydrogel healed without any external intervention, and the self-healed hydrogel can be held up (**Fig. 1e**). The self-healing property of the hydrogel was further evaluated by employing a rheometer. From the strain amplitude sweep result, the QCS2-ODex-31 hydrogel network collapsed when the strain was 50% (**Fig. 3g**). Afterwards, the continuous step strain method

was carried out to perform the rheological recovery behavior of the QCS2-ODex-31 hydrogel (**Fig. 3h**). At a high strain (100%), G´´ > G´, and G´ decreased significantly from 667 Pa to 60 Pa, indicating the network structure of QCS2-ODex-31 hydrogel was collapsed. When the hydrogel was applied at low strain (1%), G´ of the hydrogel returned to its original values immediately [43]. The cyclic test results indicated that the hydrogel network recovered efficiently. The great self-healing ability of the hydrogels is attributed to the dynamic Schiff bonds between the amine groups (QCS) and aldehyde (ODex).

The hydrogels with good injectability can be effectively filled in irregular wound areas. The hydrogels could be extruded through a 2.5 mL syringe without any clogging (**Fig. 3i**, inset graph, and **Supporting Video S1**). The injectable property of the hydrogel was further evaluated via the dependence of viscosity on shear rate with a rheometer. As shown in **Fig. 3i**, with the shear rate increasing, the viscosity of hydrogel decreases. Additionally, the rheology results indicated that all hydrogels possessed excellent self-healing abilities, shear-thinning properties and injectability (**Fig. S7**).

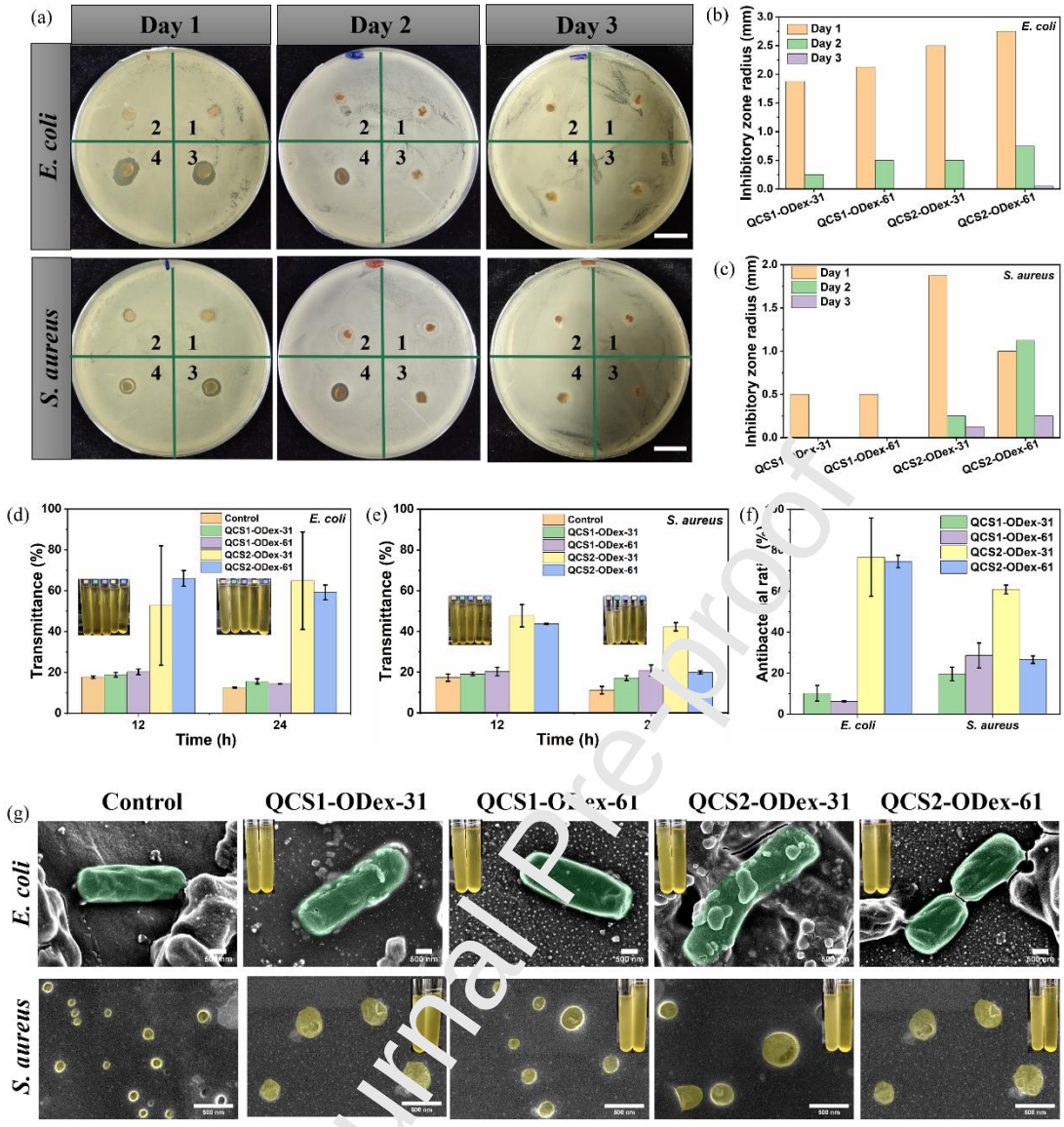

Figure 4. The antibacterial behavior of QCS-ODex hydrogels (sterilized 0.9% saline solution was taken as the control group). (**a**) Photographs of the antibacterial activity of the hydrogels against *E. coli* (gram-negative) and *S. aureus* (gram-positive) with 1, 2 and 3 days (Sample 1, 2, 3, and 4 represent QCS1-ODex-31, QCS1-ODex-61, QCS2-ODex-31, and QCS2-ODex-61 hydrogels, respectively). The inhibitory zone radius of the hydrogels against (**b**) *E. coli* and (**c**) *S. aureus* with 1, 2 and 3 days, respectively. The antibacterial behavior of the hydrogels against (**d**) *E. coli* and (**e**) *S. aureus*. (**f**) The antibacterial ratio of the hydrogels against *E. coli* and *S. aureus* for 24 h. (**g**) SEM images of *E. coli* (scale bar: 500 nm) and *S. aureus* (scale bar:

500 nm) after the hydrogels co-cultured with *E. coli* and *S. aureus* for 24 h (The bacteria were marked in different colors). Insert photograph representative that left is the control group and right is the experiment group.

3.8 *In vitro* Baicalein release

Baicalein, the main bioactive flavone of *Scutellaria baicalensis* Georgi, has been proven that possesses excellent antibacterial, anti-inflammatory, and antioxidative properties [28, 65]. Baicalein was encapsulated in QCS-ODex hydrogels to obtain Baicalein-loaded QCS-ODex hydrogels (B-QCS-ODex) (**Fig. 6a**) . The release profiles of Baicalein from the hydrogels were studied by testing the absorbance of B-QCS-ODex dipped in PBS (pH = 7.4) buffer for the different time at 275 nm with a UV-Vis spectrophotometer at 275 nm (**Fig. 6b** and **Fig. S8**).

B-QCS1-ODex hydrogels and B-QCS2-ODex hydrogels displayed a different Baicalein's release behavior (**Fig. 6c**). B-QCS2-ODex hydrogels showed faster release speed, while B-QCS1-ODex hydrogels presented a constant and stable release within 48 h. It may be attributed to higher cross-linking and tighter interconnectivity hydrogel network of B-QCS1-ODex hydrogels. The reason was also applied to explain the difference in biodegradation between B-QCS1-ODex hydrogels and B-QCS2-ODex hydrogels: after immersing in PBS (pH = 7.4) buffer for 120 h, B-QCS1-ODex hydrogels could still be kept stable shapes, B-QCS2-Odex hydrogels were degraded entirely and couldn't be observed (**Fig. 6d**). These results elucidated the sustained release behavior of baicalein from B-QCS-ODex hydrogels, and the excellent biodegradation ability was potential for adapting complex wound

healing as dressings.

3.9 Antioxidant activity

The induction of antioxidant activity has been demonstrated to present a positive effect on the wound healing process due to their regulation of the overproduction of reactive oxygen species (ROS). All hydrogels based on QCS-ODex copolymer showed an obvious decrease in intensity of DPPH peak and scavenged more than 30% DPPH (**Fig. 3f**), which was attributed to electron transfer or hydrogen atom donation from nitrogen ions segments to DPPH free radicals. Furthermore, hydrogel prepared from QCS without nitrogen ions segments as a negative control showed almost no decrease in intensity of the DPPH peak compared to that of the pure DPPH (**Fig. S9** and **Fig. S10**). The introduction of ODex was also beneficial in improving the antioxidant properties of hydrogels.

Studies proved that Baicalein, as a flavonoid drug, possesses effective antioxidant property [28, 65]. In **Fig. 6e**, B-QCS-ODex hydrogels presented enough antioxidant capacity at 0.5 h, and DPPH scavenging was higher than QCS-ODex hydrogels. The drug-loading hydrogels also can permanently maintain the antioxidant capacity, ensuring a continuous antioxidant capacity in the wound healing process. The results verified Baicalein could function as an antioxidant, making B-QCS-ODex hydrogels much more suitable for applying wound healing as dressings.

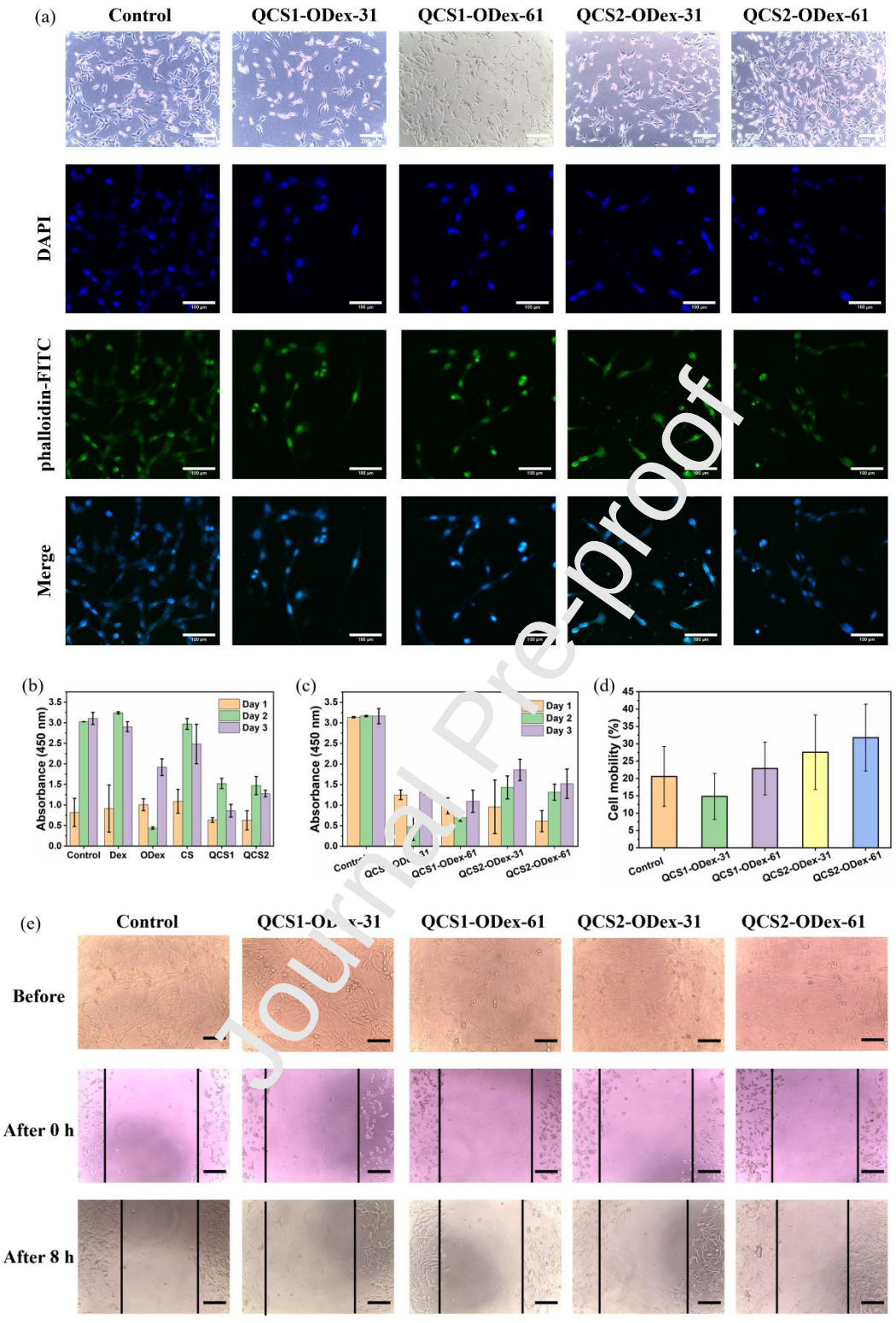

Figure 5. The biocompatibility evaluation of QCS-ODex hydrogels. (**a**) The proliferation of the NIH-3T3 cells in 24 h using the extract liquid test method. The first rank was recorded with an optical microscope (Scale bar: 200 μm), and the other rank was recorded by a laser

confocal fluorescence microscope. Blue: the cells were stained using DAPI. Green: the cells were stained using phalloidin-FITC. Scale bar: 100 μm. (**b**) (**c**) The cytocompatibility of the CS, QCS1, QCS2, Dex, ODex and hydrogels was evaluated by CCK-8 assay by culturing with NIH-3T3 cells for 1, 2, and 3 days. (**d**) Cell mobility of hydrogels. (**e**) The cell scratch test results of the cells at different times. All the black dotted lines indicate the width of the scratch gap. Scale bar: 200 μm.

3.10 Antibacterial assay

All hydrogels exhibited antimicrobial effectiveness against *S. aureus* and *E. coli*. An inhibition zone test was carried out on both *E. coli* and *S. aureus* to observe the antibacterial activity of QCS-ODex hydrogels (**Fig. 4a-c**). QCS2-containing hydrogels exhibited more excellent and permanent antibacterial properties than QCS1-containing hydrogels. Furthermore, bacterial suspension transmittance of QCS2-containing hydrogels is lower than control and QCS1-containing hydrogels, verifying its excellent antibacterial ability against *E. coli* and *S. aureus* (**Fig. 4d** and **4e**). In addition, the killing ratio was higher against *E. coli* (80%) than *S. aureus* (60%) (**Fig. 4f**); it is assigned to the structure of the cytoderm of *E. coli* and *S. aureus* is different. The morphology of bacteria was observed by SEM (**Fig. 4g**). The walls of bacteria incubated with QCS2-containing hydrogels were folded, even damaged.

The results revealed that all QCS-ODex hydrogels possessed good antibacterial activity. Especially, QCS2-containing hydrogels had effective broad-spectrum antibacterial properties and were the potential for treating complex infected wounds. The Schiff base bonds, including aromatic rings, benefit the antibacterial activity of QCS-ODex hydrogels [66]. In

QCS-ODex hydrogels, QCS with positive-charged amino groups and quaternary ammonium groups played a major role in antibacterial activity because it can damage the negative walls of bacteria by electrostatic interaction [5, 49].

B-QCS2-ODex hydrogels presented a strong antibacterial ability against *E. coli* (80%) than *S. aureus* (60%), similar to QCS-ODex hydrogels (**Fig. 6f**). The results revealed that *in situ* encapsulated Baicalein to QCS-ODex hydrogels couldn't change the antibacterial property of hydrogels.

3.11 Cytotoxicity evaluation

The cytocompatibility of hydrogels is a significant factor in the wound healing field [67]. After being co-cultured with the extracted liquid of the hydrogels for 24 h at 37 °C, NIH 3T3 cells showed normal spindle morphology (**Fig. 5a**), revealing that the hydrogels had good biocompatibility. In **Fig. 5b-c**, the optical density (OD) values (450 nm) of Dex, ODex, CS, QCS1, QCS2 and the hydrogels were increased over days, indicating they were biocompatibility. This is because the materials based on natural polysaccharides have a similar extracellular matrix, which could promote cell proliferation [68].

The pro-migration ability of QCS-ODex hydrogels was assessed using a scratch assay after removing the extract of hydrogels which co-incubation with cells for 24 h. In **Fig. 5d** and **5e**, the cell migration ability of QCS2-ODex-31 and QCS2-ODex-61 hydrogels was higher than the control group and other hydrogel groups after removing the extract of hydrogels for 8 h, and the migration rates of control, QCS1-ODex-31, QCS1-ODex-61, QCS2-ODex-31, and QCS2-ODex-61 hydrogel were 20.59%, 14.82%, 22.89%, 27.58% and 31.79%, respectively. The results indicated that QCS2-ODex-31 and QCS2-ODex-61

hydrogels could enhance cell migration and accelerate cell scratches' closure.

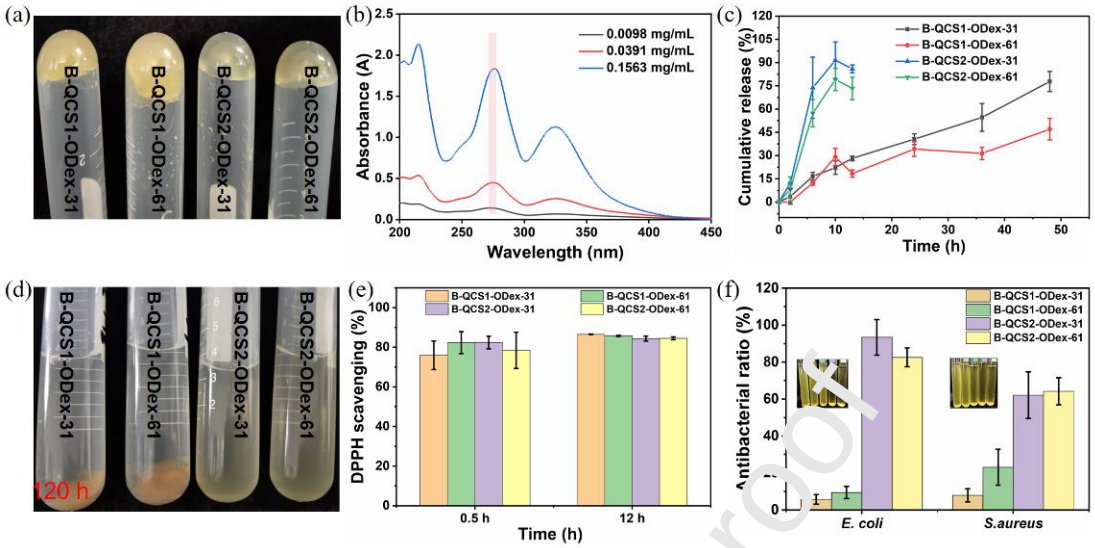

Figure 6. Characteristics of baicalein loaded hydrogels. (**a**) Photographs of baicalein-loaded hydrogels. (**b**) UV-Vis spectra of the peak of different concentration baicalein from 200 nm and 450 nm. (**c**) Baicalein release curve in PBS (pH = 7.4) buffer at 37 °C. (**d**) Degradation of the drug-loading hydrogels dipped in PBS (pH = 7.4) buffer for 120 h at 37 °C. (**e**) UV-Vis spectra of DPPH scavenging for 0.5 h and 12 h. (**f**) The antibacterial behavior and antibacterial ratio of the drug-loading hydrogels against *E. coli* and *S. aureus* for 24 h (insert photograph, the left image belongs to the control group).

3. Conclusion

A series of transparency self-healing injectable hydrogels were successfully prepared by a Schiff base reaction between amino groups of QCS and aldehyde groups of ODex under physiological conditions. These QCS-ODex hydrogels exhibited short gelation time, uniformly interconnected porous, stable storage modulus and loss modulus, suitable swelling capacity, tissue adhesion, transmission property, good self-healing, injectable, free radical

scavenging capacity, inherent antibacterial and biocompatibility. *In situ* encapsulating Baicalein into QCS-ODex hydrogels to prepare drug-loading hydrogels showed increasing antioxidant and antibacterial abilities. In summary, transparent self-healing injectable hydrogels with multifunction are ideal candidates for applying to irregular and motion wounds and observing and diagnosing the healing process as wound healing dressings.

Conflicts of Competing Interest

The authors declare no competing financial interest.

Acknowledgements

Lei Nie acknowledges the support from the Nanhu Scholars Program for Young Scholars of XYNU. The authors acknowledge the help from Prof. Lingling Wang, Prof. Qiuju Zhou, Dr. Zongwen Zhang, Dr. Dongli Xu, Zihe Jin, Lingyun Zheng, Peifang Liu, Yanping Xie, and Peiyin Guo, the Analysis & Testing Center of XYNU.

References

[1] X. Tang, X. Chen, S. Zhang, X. Gu, R. Wu, T. Huang, Z. Zhou, C. Sun, J. Ling, M. Liu, Silk-Inspired In Situ Hydrogel with Anti-Tumor Immunity Enhanced Photodynamic Therapy for Melanoma and Infected Wound Healing, Advanced Functional Materials 31(17) (2021) 2101320.

[2] X. Ding, G. Li, P. Zhang, E. Jin, C. Xiao, X. Chen, Injectable self-healing hydrogel wound dressing with cysteine-specific on-demand dissolution property based on tandem dynamic covalent bonds, Advanced Functional Materials 31(19) (2021) 2011230.

[3] Y. Cai, Z. Zhong, C. He, H. Xia, Q. Hu, Y. Wang, Q. Ye, J. Zhou, Homogeneously synthesized hydroxybutyl chitosans in alkali/urea aqueous solutions as potential wound

dressings, ACS Applied Bio Materials 2(10) (2019) 4291-4302.

[4] J. Cao, P. Wu, Q. Cheng, C. He, Y. Chen, J. Zhou, Ultrafast fabrication of self-healing and injectable carboxymethyl chitosan hydrogel dressing for wound healing, ACS applied materials & interfaces 13(20) (2021) 24095-24105.

[5] M. Li, Z. Zhang, Y. Liang, J. He, B. Guo, Multifunctional tissue-adhesive cryogel wound dressing for rapid nonpressing surface hemorrhage and wound repair, ACS applied materials & interfaces 12(32) (2020) 35856-35872.

[6] J. He, Y. Liang, M. Shi, B. Guo, Anti-oxidant electroactive and antibacterial nanofibrous wound dressings based on poly (ε-caprolactone)/quaternized chitosan-graft-polyaniline for full-thickness skin wound healing, Chemical Engineering Journal 385 (2020) 123464.

[7] L. Han, X. Lu, K. Liu, K. Wang, L. Fang, L.-T. Weng, H. Zhang, Y. Tang, F. Ren, C. Zhao, Mussel-inspired adhesive and tough hydrogel based on nanoclay confined dopamine polymerization, Acs Nano 11(3) (2017) 2561-2574.

[8] Y. Li, D. Wang, J. Wen, X. Yu, J. Liu, J. Li, H. Chu, Chemically Grafted Nanozyme Composite Cryogels to Enhance Antibacterial and Biocompatible Performance for Bioliquid Regulation and Adaptive Bacteria Trapping, Acs Nano 15(12) (2021) 19672-19683.

[9] W. Han, B. Zhou, K. Yang, X. Xiong, S. Luan, Y. Wang, Z. Xu, P. Lei, Z. Luo, J. Gao, Biofilm-inspired adhesive and antibacterial hydrogel with tough tissue integration performance for sealing hemostasis and wound healing, Bioactive materials 5(4) (2020) 768-778.

[10] E.M. Ahmed, Hydrogel: Preparation, characterization, and applications: A review, Journal of Advanced Research 6(2) (2015) 105-121.

[11] V. Brumberg, T. Astrelina, T. Malivanova, A. Samoilov, Modern Wound Dressings: Hydrogel Dressings, Biomedicines 9(9) (2021).

[12] X. Zeng, B. Chen, L. Wang, Y. Sun, Z. Jin, X. Liu, L. Ouyang, Y. Liao, Chitosan@ Puerarin hydrogel for accelerated wound healing in diabetic subjects by miR-29ab1 mediated inflammatory axis suppression, Bioactive Materials 19 (2023) 653-665.

[13] C.-Y. Zou, X.-X. Lei, J.-J. Hu, Y.-L. Jiang, Q.-J. Li, Y.-T. Song, Q.-Y. Zhang, J. Li-Ling, H.-Q. Xie, Multi-crosslinking hydrogels with robust bio-adhesion and pro-coagulant activity for first-aid hemostasis and infected wound healing, Bioactive materials 16 (2022) 388-402.

[14] L. Jin, X. Guo, D. Gao, Y. Liu, J. Ni, Z. Zhang, Y. Huang, G. Xu, Z. Yang, X. Zhang, An NIR photothermal-responsive hybrid hydrogel for enhanced wound healing, Bioactive materials 16 (2022) 162-172.

[15] X. Tang, X. Wang, Y. Sun, L. Zhao, D. Li, J. Zhang, H. Sun, B. Yang, Magnesium Oxide-Assisted Dual-Cross-Linking Bio-Multifunctional Hydrogels for Wound Repair during Full-Thickness Skin Injuries, Advanced Functional Materials 31(43) (2021) 2105718.

[16] L. Wang, X. Zhang, K. Yang, Y.V. Fu, T. Xu, S. Li, D. Zhang, L.N. Wang, C.S. Lee, A novel double-crosslinking-double-network design for injectable hydrogels with enhanced tissue adhesion and antibacterial capability for wound treatment, Advanced Functional Materials 30(1) (2020) 1904156.

[17] C. Weller, 4 - Interactive dressings and their role in moist wound management, in: S. Rajendran (Ed.), Advanced Textiles for Wound Care, Woodhead Publishing2009, pp. 97-113.

[18] B. Liu, R. Fu, Z. Duan, C. Zhu, J. Deng, D. Fan, Ionic liquid-based non-releasing antibacterial, anti-inflammatory, high-transparency hydrogel coupled with electrical

stimulation for infected diabetic wound healing, Composites Part B: Engineering 236 (2022) 109804.

[19] N. Tang, R. Zhang, Y. Zheng, J. Wang, M. Khatib, X. Jiang, C. Zhou, R. Omar, W. Saliba, W. Wu, Highly Efficient Self-Healing Multifunctional Dressing with Antibacterial Activity for Sutureless Wound Closure and Infected Wound Monitoring (Adv. Mater. 3/2022), Advanced Materials 34(3) (2022) 2270025.

[20] A.P. Dhand, J.H. Galarraga, J.A. Burdick, Enhancing biopolymer hydrogel functionality through interpenetrating networks, Trends in Biotechnology 39(5) (2021) 519-538.

[21] A. Rasool, S. Ata, A. Islam, Stimuli responsive biopolymer (chitosan) based blend hydrogels for wound healing application, Carbohydrate polymers 203 (2019) 423-429.

[22] A. Shavandi, S. Hosseini, O.V. Okoro, L. Nie, F.E. Babadi, F. Melchels, 3D Bioprinting of Lignocellulosic Biomaterials, Advanced Healthcare Materials 9(24) (2020).

[23] M. Mirzaei, O.V. Okoro, L. Nie, D.F.S. Petri, A. Shavandi, Protein-Based 3D Biofabrication of Biomaterials, Bioengineering-Basel 8(4) (2021).

[24] H. Jafari, C. Delporte, K.V. Bernaerts, G. De Leener, M. Luhmer, L. Nie, A. Shavandi, Development of marine oligosaccharides for potential wound healing biomaterials engineering, Chemical Engineering Journal Advances 7 (2021) 100113.

[25] W. Wang, Z. Zeng, L. Xiang, C. Liu, D. Diaz-Dussan, Z. Du, A.B. Asha, W. Yang, Y.-Y. Peng, M. Pan, Injectable self-healing hydrogel via biological environment-adaptive supramolecular assembly for gastric perforation healing, Acs Nano 15(6) (2021) 9913-9923.

[26] L. Zhou, Y. Xi, Y. Xue, M. Wang, Y. Liu, Y. Guo, B. Lei, Injectable self-healing antibacterial bioactive polypeptide-based hybrid nanosystems for efficiently treating

multidrug resistant infection, skin-tumor therapy, and enhancing wound healing, Advanced Functional Materials 29(22) (2019) 1806883.

[27] J. He, M. Shi, Y. Liang, B. Guo, Conductive adhesive self-healing nanocomposite hydrogel wound dressing for photothermal therapy of infected full-thickness skin wounds, Chemical Engineering Journal 394 (2020) 124888.

[28] M. Sun, S. Peng, C. Zhao, J. Huang, J. Xia, D. Ye, X. Dou, W. Hou, C. Feng, Herb-Functionalized Chronic Wound Dressings for Enhancing Biological Functions: Multiple Flavonoids Coordination Driven Strategy, Advanced Functional Materials 32(34) (2022) 2204291.

[29] P. Deng, L. Yao, J. Chen, Z. Tang, J. Zhou, Chitosan-based hydrogels with injectable, self-healing and antibacterial properties for wound healing, Carbohydrate polymers 276 (2022) 118718.

[30] P. Deng, W. Jin, Z. Liu, M. Cao, J. Zhou, Novel multifunctional adenine-modified chitosan dressings for promoting wound healing, Carbohydrate Polymers 260 (2021) 117767.

[31] M. Li, Y. Liang, J. He, H. Zhang, B. Guo, Two-pronged strategy of biomechanically active and biochemically multifunctional hydrogel wound dressing to accelerate wound closure and wound healing, Chemistry of Materials 32(23) (2020) 9937-9953.

[32] Y. Liang, M. Li, Y. Huang, B. Guo, An integrated strategy for rapid hemostasis during tumor resection and prevention of postoperative tumor recurrence of hepatocellular carcinoma by antibacterial shape memory cryogel, Small 17(38) (2021) 2101356.

[33] H. Mokhtari, M. Kharaziha, F. Karimzadeh, S. Tavakoli, An injectable mechanically robust hydrogel of Kappa-carrageenan-dopamine functionalized graphene oxide for

promoting cell growth, Carbohydr. Polym. 214 (2019) 234-249.

[34] N. Annabi, D. Rana, E. Shirzaei Sani, R. Portillo-Lara, J.L. Gifford, M.M. Fares, S.M. Mithieux, A.S. Weiss, Engineering a sprayable and elastic hydrogel adhesive with antimicrobial properties for wound healing, Biomaterials 139 (2017) 229-243.

[35] S. Tavakoli, A.S. Klar, Advanced Hydrogels as Wound Dressings, Biomolecules 10(8) (2020).

[36] G.F. Caetano, M.A. Frade, T.A. Andrade, M.N. Leite, C.Z. Bueno, M. Moraes Â, J.T. Ribeiro-Paes, Chitosan-alginate membranes accelerate wound healing, J. Biomed. Mater. Res. B Appl. Biomater. 103(5) (2015) 1013-22.

[37] G.I. Howling, P.W. Dettmar, P.A. Goddard, F.C. Hampson, M. Dornish, E.J. Wood, The effect of chitin and chitosan on the proliferation of human skin fibroblasts and keratinocytes in vitro, Biomaterials 22(22) (2001) 2959-2966.

[38] S.R. Chowdhury, V.K. Gupta, H.K. Majumder, Chapter 11 - Targeting DNA topoisomerases in parasitic protozoa by natural products: Chemical and biological perspectives, in: R. Atta ur (Ed.), Stud. Nat. Prod. Chem., Elsevier2020, pp. 389-410.

[39] J. Cho, J. Grant, M. Piquette-Miller, C. Allen, Synthesis and physicochemical and dynamic mechanical properties of a water-soluble chitosan derivative as a biomaterial, Biomacromolecules 7(10) (2006) 2845-2855.

[40] L. Nie, P. Zou, S. Feng, J. Suo, Temperature-sensitive star-shaped block copolymers hydrogels for an injection application: Phase transition behavior and biocompatibility, Journal of Materials Science: Materials in Medicine 24(3) (2013) 689-700.

[41] P. Zou, J. Suo, L. Nie, S. Feng, Temperature-sensitive biodegradable mixed star-shaped

block copolymers hydrogels for an injection application, Polymer 53(6) (2012) 1245-1257.

[42] H. Jafari, P. Ghaffari-Bohlouli, D. Podstawczyk, L. Nie, A. Shavandi, Tannic acid post-treatment of enzymatically crosslinked chitosan-alginate hydrogels for biomedical applications, Carbohydrate Polymers 295 (2022) 119844.

[43] X. Zhao, H. Wu, B. Guo, R. Dong, Y. Qiu, P.X. Ma, Antibacterial anti-oxidant electroactive injectable hydrogel as self-healing wound dressing with hemostasis and adhesiveness for cutaneous wound healing, Biomaterials 122 (2017) 34-47.

[44] P. Deng, X. Liang, F. Chen, Y. Chen, J. Zhou, Novel multifunctional dual-dynamic-bonds crosslinked hydrogels for multi-strategy therapy of MRSA-infected wounds, Applied Materials Today 26 (2022) 101362.

[45] N. Yang, S. Wang, P. Ding, S. Sun, Q. Wei, H. Jafari, L. Wang, Y. Han, O.V. Okoro, T. Wang, Magnesium-doped Biphasic Calcium Phosphate Nanoparticles with Incorporation of Silver: Synthesis, Cytotoxic and Antibacterial Properties, Mater Lett (2022) 132478.

[46] L. Nie, P. Chang, C. Ji, F. Zhang, Q. Zhou, M. Sun, Y. Sun, C. Politis, A. Shavandi, Poly (acrylic acid) capped iron oxide nanoparticles via ligand exchange with antibacterial properties for biofilm applications, Colloids and Surfaces B: Biointerfaces 197 (2021) 111385.

[47] L. Nie, Y. Deng, Y. Zhang, Q. Zhou, Q. Shi, S. Zhong, Y. Sun, Z. Yang, M. Sun, C. Politis, Silver-doped biphasic calcium phosphate/alginate microclusters with antibacterial property and controlled doxorubicin delivery, Journal of Applied Polymer Science 138(19) (2021) 50433.

[48] Y. Huang, L. Mu, X. Zhao, Y. Han, B. Guo, Bacterial Growth-Induced Tobramycin

Smart Release Self-Healing Hydrogel for Pseudomonas aeruginosa-Infected Burn Wound Healing, Acs Nano 16(8) (2022) 13022-13036.

[49] B. Zhang, J. He, M. Shi, Y. Liang, B. Guo, Injectable self-healing supramolecular hydrogels with conductivity and photo-thermal antibacterial activity to enhance complete skin regeneration, Chemical Engineering Journal 400 (2020) 125994.

[50] X. Zhang, Y. Yang, J. Yao, Z. Shao, X. Chen, Strong collagen hydrogels by oxidized dextran modification, Acs Sustain Chem Eng 2(5) (2014) 1318-1324.

[51] X. Zhao, P. Li, B. Guo, P.X. Ma, Antibacterial and conductive injectable hydrogels based on quaternized chitosan-graft-polyaniline/oxidized dextran for tissue engineering, Acta biomaterialia 26 (2015) 236-248.

[52] J. Qu, X. Zhao, Y. Liang, T. Zhang, P.X. Ma, B. Guo, Antibacterial adhesive injectable hydrogels with rapid self-healing, extensibility and compressibility as wound dressing for joints skin wound healing, Biomaterials 183 (2018) 185-199.

[53] Y. Chen, D. Wang, A. Mensaha, Q. Wang, Y. Cai, Q. Wei, Ultrafast gelation of multifunctional hydrogel composite based on self-catalytic Fe3+/Tannic acid-cellulose nanofibers, J. Colloid Interface Sci. 606 (2022) 1457-1468.

[54] L. Zhang, M. Liu, Y. Zhang, R. Pei, Recent progress of highly adhesive hydrogels as wound dressings, Biomacromolecules 21(10) (2020) 3966-3983.

[55] S. Liu, Y. Zhao, H. Wei, L. Nie, P. Ding, H. Sun, Y. Guo, T. Chen, O.V. Okoro, A. Shavandi, Injectable hydrogels based on silk fibroin peptide grafted hydroxypropyl chitosan and oxidized microcrystalline cellulose for scarless wound healing, Colloids and Surfaces A: Physicochemical and Engineering Aspects (2022) 129062.

[56] J.-f. Pan, N.-h. Liu, H. Sun, F. Xu, Preparation and Characterization of Electrospun PLCL/Poloxamer Nanofibers and Dextran/Gelatin Hydrogels for Skin Tissue Engineering, PLOS ONE 9(11) (2014) e112885.

[57] J.W. Kim, M.J. Kim, C.S. Ki, H.J. Kim, Y.H. Park, Fabrication of bi-layer scaffold of keratin nanofiber and gelatin-methacrylate hydrogel: Implications for skin graft, Int. J. Biol. Macromol. 105 (2017) 541-548.

[58] J. Xu, Y. Liu, S.-h. Hsu, Hydrogels based on Schiff base linkages for biomedical applications, Molecules 24(16) (2019) 3005.

[59] S. Li, M. Pei, T. Wan, H. Yang, S. Gu, Y. Tao, X. Liu, Y. Zhou, W. Xu, P. Xiao, Self-healing hyaluronic acid hydrogels based on dynamic Schiff base linkages as biomaterials, Carbohydrate polymers 250 (2020) 116922.

[60] C. Wang, X. Jiang, H.-J. Kim, S. Zhang, X. Zhou, Y. Chen, H. Ling, Y. Xue, Z. Chen, M. Qu, Flexible patch with printable and antibacterial conductive hydrogel electrodes for accelerated wound healing, Biomaterials 285 (2022) 121479.

[61] T. Miyazaki, A. Iwamiga, Y. Shirosaki, M. Kawashita, In situ synthesis of magnetic iron oxide nanoparticles in chitosan hydrogels as a reaction field: Effect of cross-linking density, Colloids and Surfaces B: Biointerfaces 179 (2019) 334-339.

[62] W.H. Elliott, W. Bonani, D. Maniglio, A. Motta, W. Tan, C. Migliaresi, Silk hydrogels of tunable structure and viscoelastic properties using different chronological orders of genipin and physical cross-linking, ACS applied materials & interfaces 7(22) (2015) 12099-12108.

[63] H. Liu, Z. Li, S. Che, Y. Feng, L. Guan, X. Yang, Y. Zhao, J. Wang, A.V. Zvyagin, B. Yang, A smart hydrogel patch with high transparency, adhesiveness and hemostasis for

all-round treatment and glucose monitoring of diabetic foot ulcers, Journal of Materials Chemistry B 10(30) (2022) 5804-5817.

[64] W.Y. Seow, G. Salgado, E.B. Lane, C.A.E. Hauser, Transparent crosslinked ultrashort peptide hydrogel dressing with high shape-fidelity accelerates healing of full-thickness excision wounds, Sci Rep-Uk 6(1) (2016) 32670.

[65] F. Lin, Z. Wang, L. Xiang, L. Wu, Y. Liu, X. Xi, L. Deng, W. Cui, Transporting Hydrogel via Chinese Acupuncture Needles for Lesion Positioning Therapy, Advanced Science 9(17) (2022) 2200079.

[66] M.S. Mohy Eldin, E.A. Soliman, A.I. Hashem, T.M. Tamer, Antimicrobial activity of novel aminated chitosan derivatives for biomedical applications, Advances in Polymer Technology 31(4) (2012) 414-428.

[67] J.H. Teoh, A. Mozhi, V. Sunil, S.M. Tay, J. Fuh, C.-H. Wang, 3D Printing Personalized, Photocrosslinkable Hydrogel Wound Dressings for the Treatment of Thermal Burns, 31(48) (2021) 2105932.

[68] M. Hamidi, O.V. Okoro, P.B. Milan, M.R. Khalili, H. Samadian, L. Nie, A. Shavandi, Fungal exopolysaccharides: Properties, sources, modifications, and biomedical applications, Carbohydrate polymers (2022) 119152.

Declaration of interests

☒ The authors declare that they have no known competing financial interests or personal relationships that could have appeared to influence the work reported in this paper.

☐The authors declare the following financial interests/personal relationships which may be considered as potential competing interests:

No potential conflicts of financial interests/personal relationships were reported by all-authors.

.